Fabrication and luminescence properties of self-assembled CdTe quantum dots embedded in an MnTe matrix

P. Wojnar,[1,2] J. Suffczyński,[3] A. Golnik,[3] A. Ebbens,[4] U. Woggon,[4] G. Karczewski,[1] and J. Kossut[1,5]
[1]*Institute of Physics, Polish Academy of Sciences, Al. Lotników 32/46, 02-668 Warsaw, Poland*
[2]*CEA-CNRS Group "Nanophysique et Semiconducteurs," Institute Néel, Université J. Fourier, 25 Avenue des Martyrs, F-38054 Grenoble, France*
[3]*Institute of Experimental Physics, Warsaw University, Hoża 69, 00-681 Warsaw, Poland*
[4]*Experimentelle Physik IIb, University of Dortmund, Otto-Hahn Str 4, D44-221 Dortmund, Germany*
[5]*ERATO Semiconductors Spintronics Project, Al. Lotników 32/46, 02-668 Warsaw, Poland*
(Received 6 October 2009; published 25 November 2009)

The growth of self-assembled CdTe quantum dots embedded in cubic MnTe by molecular beam epitaxy is reported. The dots are forced to form despite a small lattice mismatch of 2.3% between the dot and the barrier materials. Their properties are studied by means of time integrated and time resolved photoluminescence at various temperatures and magnetic fields. We demonstrate a considerable diffusion of Mn ions from the MnTe barrier into nominally nonmagnetic CdTe quantum dot, which is manifested as an enhancement of their magneto-optical effects, such as the Zeeman splitting of excitonic levels in the dots.

DOI: 10.1103/PhysRevB.80.195321 PACS number(s): 78.67.Hc, 75.50.Pp, 75.75.+a

I. INTRODUCTION

Quantum dots (QDs) containing a fraction of transition metal ions, i.e., diluted magnetic quantum dots, exhibit simultaneously the properties of diluted magnetic semiconductors[1] (DMS) and zero dimensional structures.[2] The carriers confined within the dots interact strongly via sp-*d* exchange interaction with a finite and relatively small number of magnetic ions, which results in a giant Zeeman splitting of excitonic levels.[3–8] Therefore, diluted magnetic quantum dots offer the unique possibility of manipulation of the spin of carriers confined on a nanometer-scale volume, and may have applications in future spintronic nanodevices.[9]

The majority of attempts to introduce magnetic ions into zero-dimensional structures rely on diffusion effects, in particular, on the diffusion of magnetic ions from a diluted magnetic barrier,[3] or from a thin layer composed of DMS deposited either directly before the QDs layer,[6,10] or separated from the dots by a nonmagnetic spacer.[11,12] In other reports, the magnetic ions are introduced directly into the dots.[4,5,7,8]

In contrast to previous reports, we use the magnetic semiconductor MnTe with an antiferromagnetic spin ordering[13] (type III) as the barrier material for CdTe QDs. Despite a huge number of Mn ions present in our structure, only few of them can be influenced by an external magnetic field. Most of them are frozen in the antiferromagnetic structure of MnTe and do not contribute to any of the magneto-optical effects observed in our structure. Only the spins of Mn ions that have not any near magnetic neighbors exhibit a paramagnetic character and can be aligned by the external magnetic field. This feature highlights the Mn ions that are placed inside the CdTe QDs due to diffusion from the barrier.

Since in our structure, only two kinds of cations are involved, manganese and cadmium, the observation of the giant Zeeman splitting within CdTe QDs provides us with a tool to study the Mn diffusion. This was not obvious in the structures studied previously, which contained three cations, e.g., CdMnTe/ZnTe,[6,8,14] CdMnSe/ZnSe,[4,10,15] and CdMnTe/CdMgTe[7,16] QDs, because there was only little information about the diffusion of nonmagnetic cations, zinc, or magnesium, into the dots.

There are, however, also some disadvantages of the use of CdTe/MnTe material system for the QDs formation, such as the small lattice mismatch between cubic MnTe and CdTe of 2.3% compared to other material systems frequently used for the QDs formation, such as GaAs/InAs, 6.7%, or CdTe/ZnTe, 5.8%. The second obstacle may be the presence of the internal manganese transition, which appears at 2.0–2.1 eV and is expected to be particularly strong in our structure, due to the huge number of Mn ions present in the 1 μm-thick MnTe barrier layer. This transition causes a strong decrease in the photoluminescence (PL) intensity[17,18] and the PL-decay time[19] and affects the excitonic emission, which is at an energy above that of the manganese transition. This means that only the exciton emission at an energy below the internal manganese transition can be observed in the PL measurements.

II. SAMPLES AND EXPERIMENTS

MnTe crystallizes spontaneously in the NiAs structure, whereas the growth of the zinc blende phase is possible only by using nonequilibrium growth methods, such as, e.g., molecular beam epitaxy.[20] In order to obtain a proper epitaxial deposition of zinc blende MnTe, one has to use a substrate with a zinc blende structure,[20] a relatively high growth temperature of 350 °C and a Mn/Te flux ratio on the order of 1/10. In our particular case, we use a hybrid substrate consisting of a 4 μm-thick zinc blende CdTe layer deposited on top of GaAs-(100) commercial substrate. The growth of MnTe is monitored by reflection of high energy electron diffraction (RHEED), which shows a streaky image, proving true epitaxial deposition of this material has been achieved. After the growth of 1 μm MnTe, the substrate temperature is decreased to 300 °C and six monolayers of CdTe are deposited by alternatively opening the Cd and Te effusion cell

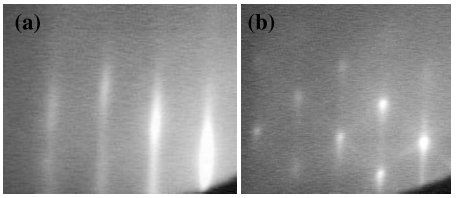

FIG. 1. The 2D-3D growth mode transition typical for the formation of self-assembled QDs in the RHEED pattern: (a) 2D surface after the deposition of 6-ML CdTe on MnTe barrier and (b) the formation of 3D islands after coverage and thermal desorption of a tellurium layer.

for 5 s. The process of QDs formation from the CdTe layer is induced by covering the surface with an tellurium layer at low substrate temperature and its subsequent thermal desorption.[21] As a consequence, the RHEED image exhibits a two-dimensional (2D)–three-dimensional (3D) growth mode transition, which directly indicates the formation of 3D islands on the surface (Fig. 1). Finally, the structure is capped with 100 nm of MnTe. A reference sample consisting of a ~ 1 μm-thick MnTe layer is grown at the same growth process. The only difference, as compared to the main sample, is that it is covered by the main shutter during the deposition of six monolayers of CdTe and, thus, does not contain any QDs.

For the micro-PL measurements, we excite and collect emission with use of an immersion reflection objective, which results in a reduction in the size of the excitation spot down to 1 μm. The photoluminescence is excited at an energy below the energy gap of MnTe at 514 nm (2.41 eV). The excitation power amounts only to 1.6 $\mu W/\mu m^2$ in order to reduce heating effects. For the detection of the PL signal, we use a charge coupled device camera coupled to a monochromator with a grating of 1200 grooves/mm. An external magnetic field up to 6 T is generated in a split coil superconducting magnet and is applied in the Faraday geometry. The sample is immersed in pumped helium where the temperature is kept constant at $T=2$ K. In the case of the time resolved PL measurements, a frequency doubled Ti:Sapphire laser system providing 150-fs laser pulses at 410 nm (3.0 eV) with a repetition rate of 75.4 MHz in conjunction with a Hamamatsu streak camera is used.

III. PHOTOLUMINESCENCE

A typical PL spectrum at 10 K of the sample containing QDs consists of two lines: the high energy line (HL) at 2.1 eV, and the low energy line (LL) at 1.8 eV (Fig. 2). In comparison, the spectrum of the reference MnTe sample includes only the high energy line. Therefore, we conclude that LL is attributed to the emission from CdTe QDs, whereas HL is related to the optical internal manganese transition. The zero-dimensional origin of LL is confirmed in this report by the high stability of the PL-intensity and PL-decay times at elevated temperatures, as well as by micro-PL measurements at an external magnetic field.

A. Temperature dependence of the photoluminescence

The spectral positions and the integrated PL-intensities for both lines, HL and LL, are determined as a function of

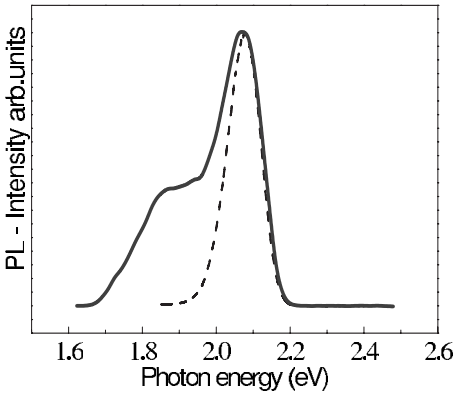

FIG. 2. PL spectrum at 10 K from the sample containing CdMnTe/MnTe QDs, solid line, and from a reference sample, containing 1 μm-thick MnTe layer, dashed line. Excitation at energy below the energy gap of MnTe, 442 nm (2.80 eV). The high energy line (HL) is attributed to the intra-Mn^{++} transition, the low energy line (LL) to the emission from the QDs. Both spectra are normalized, so that we can do the comparison between them.

the temperature. The spectral position of HL, presented in Fig. 3, shows a clear minimum at 60 K, which is a well-known feature of the internal-Mn^{++} transition, associated with the lattice constant being a function of temperature.[22] In contrast, LL shows a continuous red shift with increasing temperature, faster than expected from Varshni's law. This is a well-known feature[23] of PL lines coming from a QDs ensemble. With an increasing temperature, the carriers escape from relatively small QDs and the radiative recombination takes place only in relatively large QDs, i.e., those dots with a relatively large quantum confinement that emit photons at relatively low energies. This effect leads effectively to an additional red shift in the PL line from QDs ensemble with increasing temperature.

From the decrease in the integrated PL intensity with an increasing temperature, the thermal activation energy of nonradiative processes, E_A, is extracted by following the well-established method described, e.g., in Refs. 23 and 24. Its value amounts to 145 meV for LL and 23 meV for HL.

The relatively high value of E_A obtained for LL is consistent with results obtained for CdTe QDs embedded in a very thin MgTe layer,[25] i.e., a semiconductor with a similar energy

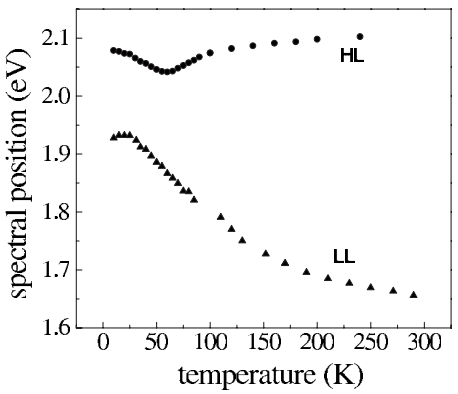

FIG. 3. Temperature dependence of the spectral position of HL and LL. Excitation line 442 nm (2.80 eV).

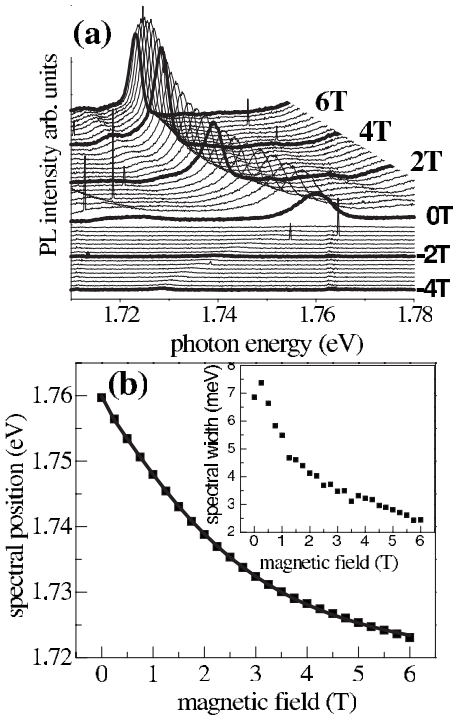

FIG. 4. (a) A typical PL line attributed to the emission from an individual QD at an external magnetic field. The red shift and circular polarization of this line prove the presence of the giant Zeeman splitting within the dot. $T=2$ K, magnetic field applied in Faraday geometry. (b) The spectral position of the PL line determined from a fit with a Gaussian vs magnetic field. Solid line—fit with a modified Brillouin function [Eq. (1)] with parameters [Eq. (2)] $E_S=41$ meV $T_{eff}=5.6$ K. Inset: the decrease in the spectral width of this PL line with an increasing magnetic field.

gap as the cubic MnTe. In this case, $-E_A=160$ meV. It is also consistent with other reports,[26,27] where an increase of E_A from CdTe/ZnMgTe QDs with an increasing Mg content in the ternary barrier has been reported. Therefore, we may conclude, that the high thermal stability of the PL emission confirms the zero-dimensional character of the low energy line.

B. Time resolved photoluminescence

The PL-decay time of LL does not depend strongly on the emission energy, as typical for self-assembled QDs,[16] and amounts typically to 300–400 ps at 10 K. These values are comparable to those obtained for nonmagnetic CdTe/ZnTe QDs (Ref. 28) and consistent with previous reports,[6] in which the emission from CdMnTe QDs lies below the intra-Mn^{++} transition. The PL-decay times do not change significantly for temperatures up to 60 K, which is also a signature of the zero-dimensional character of the structure. In the spectral range corresponding to HL, a new long living component appears, which is manifested as a constant background in the time scale under investigation and confirms that this line originates from the long living optical intra-Mn^{++} transition, which is expected to exhibit a decay constant on the order of 10 μs.[36]

C. Magnetic field dependence of the photoluminescence

The zero-dimensional origin of LL is also confirmed by the micro-PL measurements at an external magnetic field. After decreasing the excitation spot down to 1 μm, LL splits into several sharp lines with the spectral width on the order of few meV, associated with emission from individual QDs. At an external magnetic field, we observe a clear red shift in these lines ranging from 20 to 40 meV at 6 T depending on the observed line, as exemplified in Fig. 4(a). Moreover, we observe a strong circular polarization of the whole PL emission at energies corresponding to LL. The spectrum is already fully polarized at 0.2 T, which is manifested in Fig. 4(a) as a drop of the PL intensity when negative magnetic fields are applied in the Faraday geometry. Both effects are typical for structures consisting of diluted magnetic semiconductors, and prove that a giant Zeeman splitting of excitonic levels occurs within the dots. This effect is caused by the strong exchange interaction of the excitons with magnetic Mn ions and clearly demonstrates a considerable diffusion of Mn ions from the barrier into the nominally nonmagnetic CdTe QDs.

The shape of the PL lines from individual QDs can be well-fitted with a Gaussian at any magnetic field. In Fig. 4(b), we present the magnetic field dependence of the spectral position and the spectral width determined from such fits for the particular PL line under investigation. Let us first consider the spectral width dependence on the magnetic field, presented in the inset of Fig. 4(b). It amounts to 7 meV at 0 T and exhibits a clear decrease with an increasing magnetic field down to 2 meV at 6 T. As already well-established, the broadening of the PL-lines width from a diluted magnetic quantum dot is caused mostly by the magnetization fluctuations within the dot.[3,7,8,29] With an increasing magnetic field, these fluctuations are continuously reduced. This fact clearly demonstrates the paramagnetic character of Mn ions, which are responsible for the giant Zeeman splitting of the excitonic levels in our structure. Moreover, we conclude that the Mn ions, which come into the dots due to diffusion from the barrier, are mostly responsible for the magneto-optical effects observed in our structures, since the spins of Mn ions from the MnTe barrier are aligned antiferromagnetically at temperatures below 60 K.[13]

The spectral widths do not reach values typical for nonmagnetic quantum dots even at 6 T, which may reflect the fact that the spins are still far from the full alignment due to the contribution of antiferromagnetic ion-ion exchange interaction, which prevents the Mn spins from being fully aligned by the external magnetic field.[30] This explanation is further supported by the fact that the PL line position does not reach the saturation values even at 6 T and that the effective temperatures of the Mn sublattice are higher than the real temperature of the measurement.

The red shift in the spectral position of the PL lines in an external magnetic field can be well-described by a modified Brillouin function.[31] A typical fit is shown in Fig. 4(b).

$$\Delta E(B,T) = E_S \cdot B_S\left(\frac{g_{Mn}\mu_B B}{k(T_{eff})}\right) \quad (1)$$

ΔE is the energy shift, B_S the Brillouin function, B the magnetic field, $g_{Mn}=2$ the Lande factor for Mn ions, and μ_B

$=0.057$ meV$/T$ is the Bohr's magneton. There are two fitting parameters E_S and T_{eff}. E_S describes the energy shift at saturation, i.e., in case when all Mn spins are fully aligned by the magnetic field, whereas T_{eff} is the effective temperature of the Mn sublattice. They are given by the following expressions:

$$E_S = \frac{(N_0\alpha - N_0\beta)}{2} \cdot \int S_0(x_{Mn}) x_{Mn}(\vec{r}) |\Psi(\vec{r})|^2 d\vec{r},$$

$$T_{eff} = T + T_0. \quad (2)$$

$N_0\alpha$, $N_0\beta$ are the sd, pd exchange integrals, respectively, $x_{Mn}(\vec{r})$ is the Mn concentration that depends on the position within the dot, $\Psi(\vec{r})$ is the excitonic wave function, and T temperature of Mn sublattice. Both S_0 are the effective spin of an Mn ion and T_0, the contribution to the effective temperature, are phenomenological parameters influenced by several effects, such as the antiferromagnetic interaction between Mn ions,[31] or changes in the exchange integrals depending on the position of the Mn ions within the dot and the size of the dot.[32,33]

For the particular line presented in Fig. 4(b), we have obtained the fitting parameters $E_S=41$ meV and $T_{eff}=5.6$ K. In order to estimate the impact of the Mn diffusion from the barrier, we have assumed in the first step a homogenous Mn distribution within the dots and a negligible penetration of the carrier's wave functions into the barrier., The observed energy shift at magnetic field corresponds, in this case, to the average Mn content in the dot of 0.05. It is important to note that the good description of the experimental results with the modified Brillouin function confirms the paramagnetic character of Mn ions, which are responsible for the giant Zeeman splitting.

In our further considerations, we will study the magnetic field dependence of the spectral position of 18 individual QD transitions present at different parts of the PL emission spectrum. All these dependencies are fitted with the modified Brillouin function. In Fig. 5(a), we present the values of the energy shift at saturation, E_S, from these lines plotted against their spectral position at 0 T. The values of E_S range from 20 to 50 meV. Moreover, one observes an increase in the energy shift in the emission energy range from 1.7 to 1.8 eV, and a decrease from 1.8 to 1.9 eV. On the other hand, the effective temperature T_{eff}, presented in Fig. 5(b), exhibits a clear increase with increasing emission energy in the whole emission range under consideration.

We are aware that the values of E_S may be underestimated because of the presence of the magnetic polaron (MP) effect.[7,8,34] In order to estimate the impact of this effect, we have performed excitation power dependence measurements of the micro-PL at 0 T. The increase in the excitation power results in an effective increase in the temperature of the Mn sublattice. The MP effect is expected then to be manifested as an energy blue shift in the PL line from an individual QD with increasing excitation power caused by the destroying of the spin ordering of Mn ions in MP.[34] The observed blue shift in the PL lines position amounts, however, only to ~ 1 meV as the excitation power is increased by two orders of magnitude, from 1 to 100 μW$/\mu$m^2, which is a small value as compared to the energy shift at magnetic field, 20–40 meV at 6 T. Therefore, we may conclude that the fit with a Brillouin function is a good approximation for the description of the magnetic field dependences of the PL line positions.

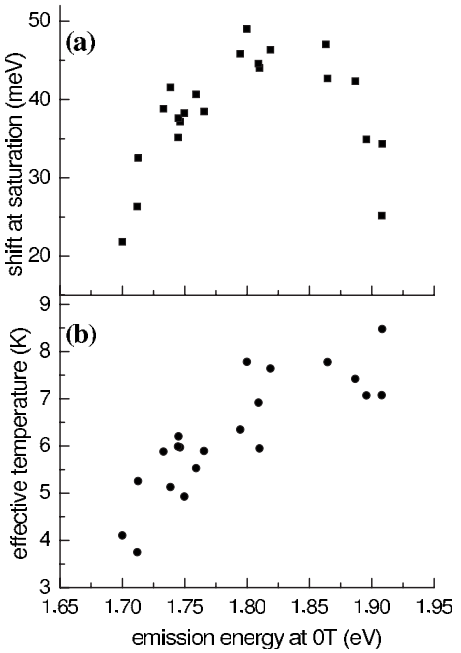

FIG. 5. (a) Energy shifts at saturation, E_S, (b) effective temperature, T_{eff} of 18 PL lines from individual QDs vs their spectral position at 0 T determined from the fits with the Brillouin function.

The results presented in Figs. 5(a) and 5(b) can be qualitatively described making a natural assumption that the diffusion of Mn ions from the barrier leads to an inhomogeneous distribution of Mn ions within the dots. The Mn concentration is expected to be enhanced at the interface of the QD and to decrease toward the center of the dot. The excitons localize then on the areas with the smallest Mn content. With a decreasing size of the quantum dots, and therefore, with an increasing emission energy, the excitonic wave function overlaps more and more with the interface region, where the Mn content is increased significantly. Consequently, the increase in the parameter E_S observed in the emission energy range from 1.7 to 1.8 eV [Fig. 5(a)] is related to the increasing overlap between the excitonic wave function and the Mn ions from the interface. A further decrease in the size of the dot makes the carrier's wave function penetrate deep into the barrier, i.e., into a region where the Mn content is very high, close to 1. In case, however, when a Mn ion has another Mn ion at the nearest neighbor position, their spins do not contribute to the total magnetization, because they are aligned antiferromagnetically with respect to each other due to the strong ion-ion exchange interaction. This leads to an effective decrease in the total magnetization[35] and, therefore, to the decrease in the energy shift at saturation, which is observed in the emission energy range from 1.8 to 1.9 eV [Fig. 5(a)].

The increasing impact of the antiferromagnetic Mn-Mn interaction is also clearly visible in Fig. 5(b), where the ef-

fective temperature is plotted vs the emission energy. As already well-established,[35] the antiferromagnetic Mn-Mn interaction leads to an effective increase in the temperature determined from the fits with a Brillouin function. A straightforward explanation of this effect is that, this interaction prevents Mn ions from being aligned by the external magnetic field. This effect has been indeed observed in Fig. 5(b), where a clear increase in the effective temperature with the increasing emission energy is reported.

It is also important to note that the emission energy of excitons is given not only by the size of the dot, as it is assumed in the above explanation, but also by the Mn content and Mn distribution inside the dots. The emission energy is expected to increase linearly with an increasing Mn content.[35] This fact, however, is also consistent with our interpretation, because in the CdTe/MnTe QDs system, the size of the dots is correlated with the Mn content inside the dots. Excitons localized in relatively large QDs interact with relatively small number of Mn ions and emit photons at relatively low energy, whereas the emission from relatively small QDs with the excitonic wave function penetrating deep into the barrier, i.e., interacting with a large number of Mn ions, takes place in the high energy part of the PL spectrum.

In order to model the results presented in Figs. 5(a) and 5(b), we have applied a theoretical attempt, which has been successfully used to describe the Mn diffusion effects in diluted magnetic quantum wells.[31] This model takes into account the Mn segregation in the growth direction during the deposition of the CdTe layer on the MnTe barrier. We obtain, as result, an exponential interface profile in the growth direction, whereas the Mn content in the consecutive monolayers amounts to 1, 1/2, 1/4, 1/8, etc. It is important to note that this interface profile is exactly the same independently of the size of the dots. This leads to an effective increase in the Mn content at the central part of relatively small dots as compared the relatively large dots. Moreover, we have assumed that this process is the main source of Mn ions inside the dots. The lateral confinement potential is assumed to be parabolic, whereas the height to diameter ratio of the dots is constant and amounts to 1/10. Therefore, the lateral confinement is manifested only as a slight increase in the calculated emission energy and does not have any impact on the magnetic properties of the dot.

The model calculations reproduce only qualitatively the results presented in Figs. 5(a) and 5(b). In particular, they reproduce such effects as the increase of E_S in a certain emission energy range, a decrease in this parameter while increasing further the emission energy, and a continuous increase of the T_{eff} in the whole emission energy range. The calculated maximal value of E_S amounts, however, only to 25 meV and the emission energy corresponding to this maximum – to 2.4 eV. This is not consistent with the experimental data, presented in Fig. 5(a), where the maximal value of E_S is around 45 meV and the corresponding emission energy amounts to 1.8 eV. We conclude, therefore, that the inhomogeneous distribution of Mn ions inside the dots gives us indeed a possibly explanation of the results presented in Figs. 5(a) and 5(b), but the segregation model[31] does not reproduce properly the Mn distribution within the dots. Most probably, we have also to take into account the lateral diffusion of Mn ions into the QDs. In order to model this lateral potential in a proper way, one needs, however, to have more knowledge about the exact sizes, shapes and strains within the dots and also about all possible migration processes of Mn ions during the formation of quantum dots.

IV. CONCLUSIONS

In summary, self-organized quantum dots CdMnTe/MnTe are successfully grown by molecular beam epitaxy despite the small lattice mismatch of 2.3% between the barrier and QDs material. The PL from this structure is visible only in the spectral range below the intra-Mn^{++} transition and exhibits a relatively high thermal stability, characterized by a thermal activation energy of nonradiative processes of $E_A = 145$ meV. In case of micro-PL measurements, the emission from the QDs splits into a series of sharp lines with the spectral width of several meV related to the emission from individual diluted magnetic QDs. In an external magnetic field up to 6T, these lines exhibit a considerable red shift in the order of ~ 30 meV, a narrowing by a factor of ~ 3 and a strong circular polarization. These features prove clearly, that there is a considerable diffusion of Mn ions from the barrier into the dots, which results in giant Zeeman splitting of excitonic levels within the dots. The Mn ions that diffuse into the CdTe QDs exhibit a paramagnetic behavior and are mostly responsible for the giant magneto-optical effects observed in our structures. Moreover, we explain a systematic study of several PL lines from individual quantum dots in terms of an inhomogeneous distribution of Mn ions inside the QDs. The Mn concentration is expected to be enhanced at the interface of the QD and to decrease toward the center of the dot.

ACKNOWLEDGMENT

This work has been supported by SANDIE Network of Excellence and Ministry of Science and Higher Education (Poland) under Grant No. N202 050 32/1187.

[1] J. Kossut and W. Dobrowolski, in *Narrow Gap II VI Compounds for Optoelectronic and Electromagnetic Applications*, edited by P. Capper (Chapman and Hall, London, 1997).
[2] M. A. Reed, Sci. Am. **268**, 98 (1993).
[3] G. Bacher *et al.*, Phys. Rev. Lett. **89**, 127201 (2002).
[4] A. Hundt, J. Puls, and F. Henneberger, Phys. Rev. B **69**, 121309(R) (2004).
[5] S. Kuroda, Y. Terai, K. Takita, T. Takamasu, G. Kido, N. Hasegawa, T. Kuroda, and F. Minami, J. Cryst. Growth **214-215**, 140 (2000).

[6] S. Mackowski, S. Lee, J. K. Furdyna, M. Dobrowolska, G. Prechtl, W. Heiss, J. Kossut, and G. Karczewski, Phys. Status Solidi B **229**, 469 (2002).
[7] A. A. Maksimov, G. Bacher, A. McDonald, V. D. Kulakovskii, A. Forchel, C. R. Becker, G. Landwehr, and L. W. Molenkamp, Phys. Rev. B **62**, R7767 (2000).
[8] P. Wojnar, J. Suffczynski, K. Kowalik, A. Golnik, G. Karczewski, and J. Kossut, Phys. Rev. B **75**, 155301 (2007).
[9] D. Loss and D. P. DiVincenzo, Phys. Rev. A **57**, 120 (1998).
[10] L. V. Titova, J. K. Furdyna, M. Dobrowolska, S. Lee, T. Topuria, P. Moeck, and N. D. Browning, Appl. Phys. Lett. **80**, 1237 (2002).
[11] L. Besombes, Y. Leger, L. Maingault, D. Ferrand, H. Mariette, and J. Cibert, Phys. Rev. Lett. **93**, 207403 (2004).
[12] L. Maingault, L. Besombes, Y. Leger, H. Mariette, and C. Bougerol, Phys. Status Solidi C **3**, 3992 (2006).
[13] T. M. Giebultowicz, P. Klosowski, N. Samarth, H. Luo, J. K. Furdyna, and J. J. Rhyne, Phys. Rev. B **48**, 12817 (1993).
[14] S. Kuroda, N. Umakoshi, Y. Terai, and K. Takita, Physica E (Amsterdam) **10**, 353 (2001).
[15] K. Shibata, K. Takabayashi, I. Souma, J. Shen, K. Yanata, and Y. Oka, Physica E (Amsterdam) **10**, 358 (2001).
[16] G. Prechtl, W. Heiss, S. Mackowski, and E. Janik, Appl. Phys. Lett. **78**, 2140 (2001).
[17] S. Lee, M. Dobrowolska, and J. K. Furdyna, Phys. Rev. B **72**, 075320 (2005).
[18] M. Nawrocki, Y. G. Rubo, J. P. Lascaray, and D. Coquillat, Phys. Rev. B **52**, R2241 (1995).
[19] J. Seufert, G. Bacher, M. Scheibner, A. Forchel, S. Lee, M. Dobrowolska, and J. K. Furdyna, Phys. Rev. Lett. **88**, 027402 (2001).
[20] E. Janik, E. Dynowska, M. J. Bak, M. Leszczynski, W. Szuszkiewicz, T. Wojtowicz, G. Karczewski, A. K. Zakrzewski, and J. Kossut, Thin Solid Films **267**, 74 (1995).
[21] F. Tinjod and H. Mariette, Phys. Status Solidi B **241**, 550 (2004).
[22] S. Biernacki, M. Kutrowski, G. Karczewski, T. Wojtowicz, and J. Kossut, Semicond. Sci. Technol. **11**, 48 (1996).
[23] G. Karczewski, S. Mackowski, M. Kutrowski, T. Wojtowicz, and J. Kossut, Appl. Phys. Lett. **74**, 3011 (1999).
[24] W. Yang, R. R. Lowe-Webb, H. Lee, and P. C. Sercel, Phys. Rev. B **56**, 13314 (1997).
[25] S. Moehl, L. Maingault, K. Kuntheak, and H. Mariette, Appl. Phys. Lett. **87**, 033111 (2005).
[26] F. Tinjod, S. Moehl, K. Kheng, B. Gilles, and H. Mariette, J. Appl. Phys. **95**, 102 (2004).
[27] F. Tinjod, K. Kheng, J. Bleuse, and H. Mariette, Physica E (Amsterdam) **17**, 68 (2003).
[28] K. P. Korona, P. Wojnar, J. A. Gaj, G. Karczewski, J. Kossut, and J. Kuhl, Solid State Commun. **133**, 369 (2005).
[29] S. Mackowski, J. Wrobel, K. Fronc, J. Kossut, F. Pulizzi, P. C. M. Christianen, J. C. Maan, and G. Karczewski, Phys. Status Solidi B **229**, 493 (2002).
[30] P. Wojnar, J. Suffczynski, K. Kowalik, M. Aleszkiewicz, G. Karczewski, and J. Kossut, Nanotechnology **19**, 235403 (2008).
[31] J. A. Gaj, W. Grieshaber, C. Bodin-Deshayes, J. Cibert, G. Feuillet, Y. MerledAubigne, and A. Wasiela, Phys. Rev. B **50**, 5512 (1994).
[32] F. Qu and P. Hawrylak, Phys. Rev. Lett. **95**, 217206 (2005).
[33] A. Bhattacharjee, Phys. Rev. B **58**, 15660 (1998).
[34] G. Bacher *et al.*, Physica E (Amsterdam) **26**, 37 (2005).
[35] J. A. Gaj, R. Planel, and G. Fishman, Solid State Commun. **29**, 435 (1979).
[36] J. D. Park, S. Yamamoto, J. Watanaba, K. Takamura, and J. Nakamura, J. Phys. Soc. Jpn. **66**, 3289 (1997).